Fiber optic microsphere with a ZnO thin film for potential application in a refractive index sensor – theoretical study

Marzena Hirsch*

Department of Metrology and Optoelectronics, Faculty of Electronics, Telecommunications and Informatics, Gdańsk University of Technology, Narutowicza Street 11/12, 80-233 Gdańsk, Poland,

Received August 30, 2018; accepted September 24, 2018; published September 30, 2018

Abstract—Optical fiber sensors of refractive index play an important role in analysis of biological and chemical samples. This work presents a theoretical investigation of spectral response of a fiber optic microsphere with a zinc oxide (ZnO) thin film deposited on the surface and evaluates the prospect of using such a structure for refractive index sensing. A microsphere is fabricated by an optical fiber tapering method on the base of a single mode fiber. The numerical model is described and simulation was conducted to assess the influence of ZnO layer deposition on a reflected signal. The results indicate that a ZnO film improves the performance in terms of application in a refractive index sensor.

Optical sensors that are based on refractive index measurements are widely used in the analysis of biological and chemical samples [1-3]. Optical fiber sensors offer many advantages like fast response, immunity to the electromagnetic noise present at the measurement site and potential for low cost solutions.

The subject of the study was to evaluate spectral response of an in-line fiber optic interferometer fabricated in the form of a microsphere with regards to potential application in refractive index sensing. In the investigated case, a sphere is created on the tip of a single mode fiber via an optical fiber tapering method. It can be presumed that in such a case the material of the fiber core and the cladding are not mixed but the original structure of the fiber is preserved - as shown in Fig. 1, the investigated structure consists of a sphere made of the cladding material with a smaller sphere of the core material formed inside.

Most energy of light propagating in the optical fiber is confined in the fiber core. In the proposed structure the input light propagated in the core is first partially reflected at the boundary between the core sphere and cladding material and then on the external boundary of the structure. Those two boundaries form a low finesse Fabry-Pérot cavity. The intensity of a reflected signal is highly dependent on the refractive index of a surrounding medium – thus it can be used to achieve a compact, robust and potentially low-cost fiber optic senor. The interference pattern reflected from such a Fabry-Pérot interferometer can be used for integrity validation of the sensor structure, as any damage to the sphere would affect it. Additionally, this way it would be possible to measure the reference of a variation in environmental temperature and pressure, as these factors would influence the optical length of the cavity.

The application of a thin layer of zinc oxide (ZnO) as an external coating can be used to achieve increased intensity of reflected light and to extend the measurement sensing range to liquids with a refractive index close to that of the fiber (1.4÷1.5) [4-5].

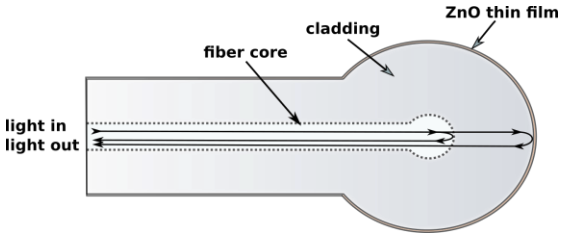

Fig. 1. Investigated microsphere interferometer.

The finesse of a Fabry-Pérot interferometer depends on mirrors reflectivity. In the investigated case, the reflection of various refractive index boundaries can be derived from Fresnel equations. However, the difference between the refractive index of the fiber core and the cladding is very small (approximately 0.006 can be assumed for a single mode fiber) thus reflection at the first cavity mirror is weak. The reflectivity of the second surface depends on the refractive index of the surrounding medium, but it is not expected to be above 0.04 for a clean sphere and 0.2 for up to 250nm ZnO coated structure [6]. In the case of such low finesse, the response of a multibeam Fabry-Pérot interferometer can be simplified by a two-beam approximation.

Figure 2 presents a schematic model of the investigated Fabry-Pérot cavity. The two beams contributing to the interference phenomena are light reflected at the fiber core-cladding boundary and light reflected at the external surface of the cladding sphere and coupled back to the fiber core.

The intensity of field distribution illuminating the end of the fiber core can be approximated by the Gaussian distribution [7]. Therefore, the field distribution of the first reflected beam can be expressed by:

* E-mail: hirsch.marzena@gmail.com

$$U_{b0}(\rho,\lambda) = r_{12}\cdot U_{in} = r_{12}\cdot A_0\cdot \exp(\tfrac{-\rho^2}{w_0{}^2}), \quad (1)$$

where ρ – the radial position ($\rho=\sqrt{x^2+y^2}$), λ – wavelength, U_{in} – amplitude of the beam incident on the cavity, w_o – fundamental mode radius of the fiber, r_{12} – Fresnel reflection coefficient of the n_1/n_2 interface.

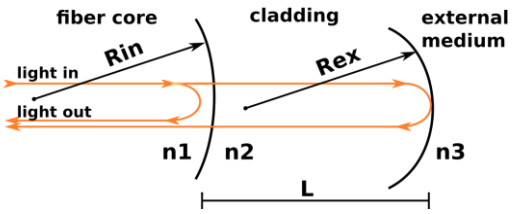

Fig. 2. Schematic model of the investigated structure.

To determine the field distribution of the second interfering beam, the transformation of the beam exiting the fiber that occurs during propagation in the cavity and reflection from the second boundary needs to be evaluated. That was performed using the ray matrices approach utilizing a complex beam parameter. Transformation matrix M can be written as [8]:

$$M=\begin{bmatrix}1 & 0\\ \frac{n_2-n_1}{n_2R_{in}} & \frac{n_1}{n_2}\end{bmatrix}\begin{bmatrix}1 & L\\ 0 & 1\end{bmatrix}\begin{bmatrix}1 & 0\\ \frac{-2}{R_{ex}} & 1\end{bmatrix}\begin{bmatrix}1 & L\\ 0 & 1\end{bmatrix}\begin{bmatrix}1 & 0\\ \frac{n_1-n_2}{n_1R_{in}} & \frac{n_2}{n_1}\end{bmatrix}, \quad (2)$$

where $n_{1,2}$ – refractive indices of the core and cladding, L - length of the cavity, $R_{in,ex}$ – radius of the core and cladding spheres respectively.

Knowing the coefficients of the transformation matrix, a complex beam parameter q_1 of the reflected light can be calculated as [8]:

$$q_1 = \frac{Aq_0+B}{Cq_0+D}, \quad (3)$$

where q_0 – complex beam parameter of the beam incident on the cavity ($q_0=(-j\lambda/\pi n_1 w_0^2)^{-1}$).

From Eq. (3) the properties of the beam (beam radius w_1 and radius of curvature R_1) the filed distribution upon exiting the cavity can be calculated [8]:

$$w_1 = \sqrt{\frac{\lambda}{\pi\cdot imag(^{-1}/_{q_1})}}, \quad (4)$$

$$R_1 = \frac{1}{real(^1/_{q_1})}, \quad (5)$$

$$U_{b1}(\rho,\lambda) = t_{12}\cdot r_{23}\cdot t_{21}\cdot \mathrm{U}_{in}\cdot\frac{w_0}{w_1}\cdot\exp\left(\frac{-\rho^2}{w_1{}^2}\right)\cdot$$
$$\cdot\exp(-j\cdot 2Lk-\frac{jk\rho^2}{2R_1}+j\cdot\mathrm{atan}(^{2L}/_{z_0})), \quad (6)$$

where $t_{12,21}$ – Fresnel transmission coefficients of n_1/n_2 boundary, r_{23} – reflection coefficient of the external surface of the microsphere, k – extinction coefficient, z_0 – Rayleigh range.

The interferometer output signal amplitude can be then calculated as:

$$U_{out}(\rho,\lambda) = U_{b0}+U_{b1}*c_{coup}, \quad (7)$$

where c_{coup} – coupling coefficient of the beams expressed by [8]:

$$c_{coup}^2 = \frac{j\cdot 2\lambda\cdot\exp\left(j\left(\frac{4\pi L n_2}{\lambda}-k2L\right)\right)}{\pi w_0 w_1(^1/_{q_0^*}-^1/_{q_1})}, \quad (8)$$

where q_0 – complex beam parameter of the first reflected beam given as [8]:

$$q_0{}^{-1} = {}^{-j\lambda}/_{\pi n_1 w_0^2}. \quad (9)$$

Intensity simulations of an output signal were performed for selected refractive index values of the surrounding media (n_3 in the range 1.0÷1.6). The radius (R_{ex}) of the microsphere was 130µm, cavity length was 110µm, refractive index of the core (n_1) was 1.46 and of the cladding (n_2) 1.454. The thickness of a ZnO film was 150 nm, the reflectance of the ZnO coated external surface of the sphere was calculated as was described in Ref. [6].

Figure 3 shows a comparison of reflected spectra obtained for a ZnO coated and a clean sphere placed in air (n_3=1.0). As can be observed, the intensity of a reflected signal for the sphere with a ZnO film is four times that of the uncoated one.

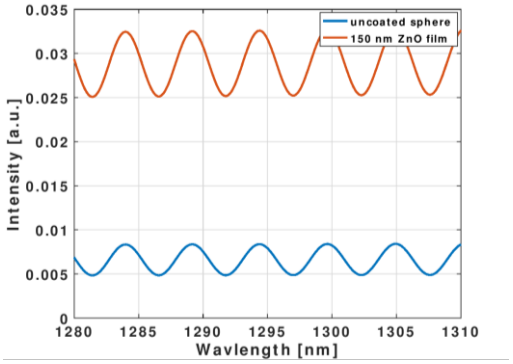

Fig. 3. Reflected spectra for an uncoated sphere and with a 150nm ZnO film.

Figures 4 and 5 present the reflected spectra obtained for selected refractive index values of the surrounding media for the sphere with a ZnO film and the uncoated one, respectively. Figure 6 shows the dependence of peak intensity in relation to the external refractive index both for the sphere with and without a deposited ZnO layer.

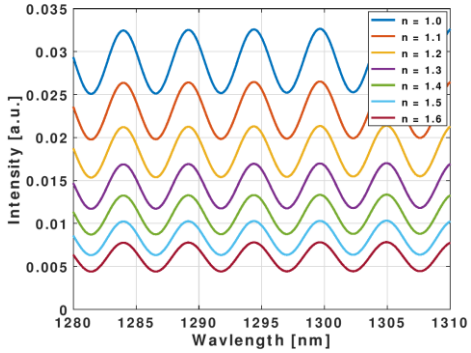

Fig. 4. Reflected spectra for the sphere with a 150nm ZnO film immersed in various refractive index liquids.

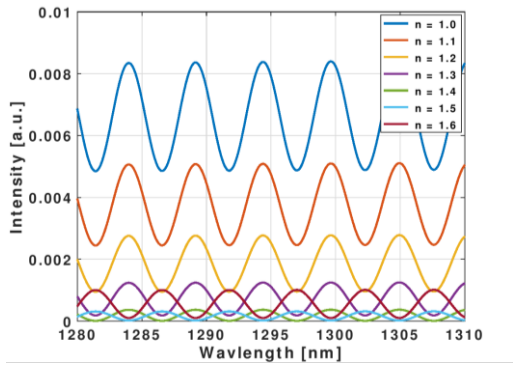

Fig. 5. Reflected spectra for the uncoated sphere immersed in various refractive index liquids.

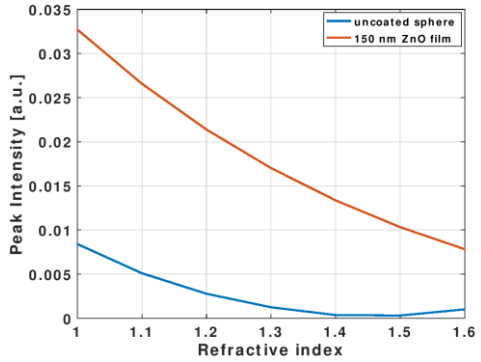

Fig. 6. Peak intensity vs. surrounding refractive index for the uncoated sphere and with a 150nm ZnO film.

As can be observed, for the structure with a ZnO film, the peak intensity is monotonically decreasing with an increasing refractive index. For the uncoated sphere, the peak intensity versus refractive index function reaches the minimum for a refractive index value between 1.4 and 1.5 due to the Fresnel reflection on the microsphere surface.

In conclusion, the results have shown that the application of a thin ZnO layer deposited on the surface of the microsphere is beneficial for the application in a refractive index sensor. In an intensity measurement-based sensor the sensitivity has improved and the range of measurement has extended from up to 1.4 achieved for the uncoated sphere to over 1.6. The extension of the measurement rage broadens the possible field of application to many substances with a refractive index close to 1.5, like benzene, toluene or various oils.

The author gratefully acknowledges the financial support from the DS funds of the Faculty of Electronics, Telecommunications, and Informatics of the Gdansk University of Technology.

References

[1] Y. Qian, Y. Zhao, Q. Wu, Y. Yang, Sens. Actuat. B: Chemical **260**, 86 (2018).
[2] M. Jędrzejewska-Szczerska, Sensors **14**(4), 6965 (2014).
[3] F. Sequeira *et al.*, Sensors **16**(12), 2119 (2016).
[4] M. Jędrzejewska-Szczerska *et al.*, Sens. Actuat. A: Physical **221**, 88 (2015).
[5] M. Hirsch, D. Majchrowicz, P. Wierzba, M. Weber, M. Bechelany, M. Jędrzejewska-Szczerska, Sensors **17**(2), 261 (2017).
[6] M. Hirsch, P. Wierzba, M. Jędrzejewska-Szczerska, Proc. SPIE **10161**, 101610D (2016).
[7] J. Pluciński, K. Karpienko, Proc. SPIE **10034**, 100340H (2016).
[8] P.F. Goldsmith, *Quasioptical systems: Gaussian beam quasi-optical propagation and applications* (Piscataway, NJ: IEEE Press 1998).

